

This item is the archived peer-reviewed author-version of:

Assessment of pool boiling correlations using experimental data with refrigerant FK-649

Reference:

T' Jollyn Ilya, Nonneman Jasper, Beyne Wim, De Paepe Michel.- Assessment of pool boiling correlations using experimental data with refrigerant FK-649
Science et technique du froid / Institut international du froid; International Institute of Refrigeration- ISSN 0151-1637 - Paris, International Institute of
Refrigeration, 26(2023), p. 558-566

Full text (Publisher's DOI): <https://doi.org/10.18462/iir.icr.2023.0521>

To cite this reference: <https://hdl.handle.net/10067/2016720151162165141>

Assessment of pool boiling correlations using experimental data with refrigerant FK-649

Ilya T'JOLLYN^{*(a,b)}, Jasper NONNEMAN^(b,c), Wim BEYNE^(b,c), Michel DE PAEPE^(b,c)

^(a) University of Antwerp

Antwerp, 2020, Belgium, research@uantwerpen.be

^(b) Ghent University

Ghent, 9000, Belgium, info@ugent.be

^(c) FlandersMake@UGent – Core lab MIRO

Leuven, 3001, Belgium, info@flandersmake.be

*Corresponding author: ilya.tjollyn@uantwerpen.be

ABSTRACT

Experimental measurements of nucleate pool boiling heat transfer of refrigerant FK-649 are compared to predictions by several correlations from scientific literature. Thirteen frequently used nucleate pool boiling heat transfer correlations were selected. Two of these correlations (the Rohsenow and Piro correlation) contain constants which need to be fitted to the specific surface-fluid combination. As expected, the correlations which contain fitting constants agree best with the data. The Rohsenow correlation is the preferred correlation, as this correlation only requires one fitting constant (the Piro correlation requires two) but has the same predictive performance as the Piro correlation. The normalized mean absolute error when comparing the measurement data to the predictions with the Rohsenow correlation is equal to 7.5%, while the maximal deviation is 25.6%. These values indicate that the fitted Rohsenow correlation matches fairly well with the measurement data. If no data is available to fit the constants, the Labuntsov correlation gave the best results. Remarkably, the normalized mean absolute error of this correlation was also equal to 7.5%, while no fitting parameters were used. The maximal deviation was equal to 29.1%, which is slightly larger than for the fitted Rohsenow correlation. The Labuntsov correlation is thus the best correlation for the prediction of heat transfer rates for pool boiling with FK-649 and works almost as well as the fitted correlations. An important drawback of the Labuntsov correlation is that it does not take into account the effect of boiling surface microgeometry. As such, it should not be used for surfaces with very high or low surface roughness.

Keywords: nucleate boiling, pool boiling, low-GWP refrigerants, two-phase heat transfer, heat transfer correlations.

1. INTRODUCTION

Nucleate pool boiling is an important mode of heat transfer in many industrial applications, such as cooling of electronic devices and power generation using (organic) Rankine cycles. Accurate predictions of heat transfer rates are critical for designing and optimizing industrial processes that involve boiling. Due to its complexity and the variety of factors that can influence the process, this can be challenging (Piro et al., 2004a). To address this challenge, researchers have developed a range of correlations that relate the heat flux to the surface superheat temperature (difference between surface temperature and fluid saturation temperature). However, it is still unclear which correlations perform best, especially for newer and not yet extensively studied fluids. One of such fluids is FK-649, which is considered a potential fluid for several applications such as two-phase electronics cooling due to its low GWP equal to 1 (Forrest et al., 2013). A downside of FK-649 is that it is considered a PFAS, for which regulations are becoming stricter due to concerns about accumulation in the environment and human health risks.

Pirotto et al. (2004b) compared the Kruzhilin, Rohsenow, Kutateladze-Borishanskii, Labuntsov, Kutateladze and Pirotto correlation to experimental data. No correlations using the theory of thermodynamic similarity are included in the comparison. The authors conclude that the Rohsenow and Pirotto correlations are most accurate. This is to be expected, as both these correlations were fitted with two parameters to the experimental data to which they are compared. They can therefore not be directly used for untested surface-fluid combinations. Of the other correlations, the Kutateladze-Borishanskii correlation renders the best prediction of the experimental data. Forrest et al. (2013) made an analysis of the Rohsenow, Borishanskii-Mostinski, Stephan-Abdelsalam, Cooper and Leiner correlations by evaluating the predictive power with regard to their experimental results. Also here, the Rohsenow correlation performed best as a result of the fitting coefficients used. Of the other correlations, Stephan-Abdelsalam performed best, followed by Leiner and Cooper, while Borishanskii-Mostinski underpredicted heat transfer rates by about 50%. Bartle et al. (2018) performed a similar analysis with the Kruzhilin, Rohsenow, Borishanskii-Mostinski, Labuntsov, Gorenflo, Stephan-Abdelsalam, Kutateladze and Leiner correlations. The Cooper correlation was not included in the analysis as the molar mass of the fluid under test was higher than the range for which the Cooper correlation was fitted. Also in this analysis, using the fitting parameters in the Rohsenow correlation resulted in the best prediction. However, the Rohsenow correlation was also compared to the experimental data when using the coefficients originally suggested. For this case, the predictive accuracy was less than the correlation of Labuntsov, which performed best of the correlations without fitting parameters. The Gorenflo correlation also provided adequate predictions while in addition taking into account the effect of surface roughness. All other correlations had significantly larger deviations from the experimental results.

It is clear that there is no consensus on which a priori correlation (without fitting constants) is most suited for predicting nucleate pool boiling heat transfer. Large deviations from measured heat transfer rates are common for all correlations, indicating that not all effects are properly taken into account and that the heat transfer mechanisms are not yet fully understood. The goal of this study is therefore to analyse which correlations are best suited to predict the nucleate pool boiling heat transfer rates of FK-649.

2. NUCLEATE POOL BOILING HEAT TRANSFER CORRELATIONS

Table 1 gives an overview of thirteen correlations which have been proposed and used in scientific literature. All parameters and symbols used in the equations can be found in the nomenclature at the end of the paper. The list of correlations in this study is by no means meant to be comprehensive. The correlations reported here are chosen on the basis of their use by other researchers. The correlations are covered chronologically with regard to the first publication that was found describing it.

The oldest correlation analysed is that of Kruzhilin (1947) and it is based on non-dimensional analysis. This correlation uses the capillary length as a parameter, which is defined by Eq. (1).

$$L_c = \sqrt{\frac{\sigma}{g(\rho_l - \rho_v)}} \quad \text{Eq. (1)}$$

The correlation by Rohsenow (1952) is one of most well-known and used correlations. It features three fitting parameters to take into account the influence of the surface-fluid combination. Typically, only the constant C_{sf} is fitted, while the parameters r and s are kept to the standard values of 0.33 and 1.7. The Forster-Zuber correlation (Forster and Zuber, 1955) was fitted only to critical heat flux data, so it is not expected to perform well for the entire heat flux range. The first correlation of Kutateladze was proposed in collaboration with Borishanskii (Kutateladze and Borishanskii, 1958). Later, Borishanskii and Mostinski proposed a correlation which determines the influence of the fluid properties solely on the critical and reduced pressure (Borishanskii, 1961 and Mostinski, 1963). In this equation, the heat flux is evaluated in $\text{W}\cdot\text{m}^{-2}$, the surface superheat in K and the critical pressure in bar. Shekriladze and Ratiani (1966) take into account the microgeometry of the boiling surface by a parameter r_c which is the effective radius of the nucleation sites. Labuntsov (1972) made a correlation based on a theoretical analysis of heat transfer in a thin liquid layer under the vapour bubbles. Gorenflo proposed a correlation which splits up the effects of heat flux, fluid, saturation pressure and surface properties, of which the most recent one is used in this study (Gorenflo and Kenning,

1990). Using a regression analysis with thirteen dimensionless groups, Stephan and Abdelsalam (1978) developed a new correlation. This correlation uses the Fritz bubble departure diameter as determined by Eq. (2).

$$D_F = 0.851\beta \sqrt{\frac{2\sigma}{g(\rho_l - \rho_v)}} \quad \text{Eq. (2)}$$

Another widely used correlation is that of Cooper (1984), which uses the reduced pressure and the fluid molar mass to take into account fluid property variations. Several decades after his first correlation, Kutateladze (1990) also proposed a second correlation, based on different dimensionless numbers. The correlation by Leiner (1994) is based on the Gorenflo correlation, but uses the critical fluid data (temperature and pressure) in the equation. Finally, Piroo et al. (2004b) propose a correlation similar to that of Rohsenow, which contains two fitting parameters: C_{sf}^* and m .

3. ASSESSMENT OF CORRELATIONS

3.1. Methodology

To assess the predictive quality of the correlations described in the previous section, the surface superheat temperatures predicted by the correlations are compared to those gathered from measurements described by T'Jollyn et al. (2019) and T'Jollyn et al. (2022). The heat transfer rate was measured for fluid FK-649 on a flat horizontal surface for two boiling surfaces: an aluminium and a copper surface. The arithmetic mean roughness of the used surfaces is equal to 0.9 μm and 0.2 μm for the aluminium and copper surfaces respectively. The applied heat flux ranges from 8 $\text{kW}\cdot\text{m}^{-2}$ to 146 $\text{kW}\cdot\text{m}^{-2}$ and the saturation temperature of the fluid was varied from 36 $^{\circ}\text{C}$ to 46 $^{\circ}\text{C}$. A total of 91 steady-state measurement points were collected.

The heat transfer correlations are assessed by determining the surface superheat temperature based on the different correlations and comparing this to the measured surface superheat temperature. Thirteen correlations for nucleate pool boiling heat transfer have been described. For the Rohsenow and Piroo correlations, two predictions are made using either a priori determined constants from other studies or by fitting the constants to the measurements of this study. This results in fifteen different heat transfer correlations to be analysed.

3.2. Inputs

All heat transfer correlations require the measured heat flux as an input parameter. Besides the heat flux, all correlations require information on the state of the fluid and/or some of the fluid properties. The state of the fluid is always at saturation and is derived from temperature and pressure measurements in the refrigerant reservoir. The potentially required fluid characteristics and properties are determined using the REFPROP program (Lemmon et al., 2018), which determines the equation of state from McLinden et al. (2015), liquid viscosity from Wen et al. (2017), liquid thermal conductivity from Perkins et al. (2018) and surface tension from Cui et al. (2018).

Several correlations use the gravitational acceleration as a parameter, which is equal to 9.81 $\text{m}\cdot\text{s}^{-2}$. If $R_{p,DIN}$ is used as a parameter, which is a roughness parameter based on the DIN 4762 standard, it is estimated as 2.5 times the arithmetic mean roughness R_a (Forrest et al., 2013). The Stephan-Abdelsalam correlation uses the static contact angle, which is assumed here equal to 35 $^{\circ}$, as is also done in the analysis of Stephan and Abdelsalam (1980) for refrigerants. This parameter was not measured, so it is merely a best guess. The Gorenflo correlation requires the property ($k_w \rho_w c_{p,w}$) of the wall material, which is 561 $\text{kJ}^2\cdot\text{m}^{-4}\cdot\text{K}^{-2}\cdot\text{s}^{-1}$ for the aluminium surface and 1250 $\text{kJ}^2\cdot\text{m}^{-4}\cdot\text{K}^{-2}\cdot\text{s}^{-1}$ for the copper surface. The Shekrladze-Ratiani correlation uses the radius of the critical nucleus as a parameter for the microgeometry of the boiling surface. As it is unclear how to determine this parameter, a value of 5 μm is used as is suggested by Shekrladze (1981). This value is used for both tested boiling surfaces.

Table 1. Nucleate pool boiling heat transfer correlations assessed in this study

| | | |
|--------------------------|--|----------|
| Kruzhilin | $\frac{\dot{q}L_c}{k_l\Delta T_s} = 0.082 \left(\frac{\dot{q}h_{lv}}{gT_{sat}k_l\rho_l - \rho_v} \right)^{0.7} \left(\frac{T_{sat}c_{p,l}\rho_l\sigma}{h_{lv}^2\rho_v^2L_c} \right)^{1/3} Pr_l^{-0.45}$ | Eq. (3) |
| Rohsenow | $\frac{c_{p,l}\Delta T_s}{h_{lv}} = C_{sf} \left[\frac{\dot{q}}{\mu_l h_{lv}} \sqrt{\frac{\sigma}{g(\rho_l - \rho_v)}} \right]^r Pr_l^s$ | Eq. (4) |
| Forster-Zuber | $\frac{\dot{q}}{\Delta T_s} = 0.0015 \frac{k_l}{\Delta T_s c_{p,l} \rho_l \sqrt{\pi \alpha_l}} \frac{1}{h_{lv} \rho_v} \frac{1}{\sqrt{\Delta p_s}} \frac{1}{\sqrt{\Delta p_s}} \left[\frac{\rho_l}{\mu_l} \left(\frac{\Delta T_s c_{p,l} \rho_l \sqrt{\pi \alpha_l}}{h_{lv} \rho_v} \right)^2 \right]^{0.62} Pr_l^{0.33}$ | Eq. (5) |
| Kutateladze-Borishanskii | $\frac{\dot{q}L_c}{k_l\Delta T_s} = 0.00071 Pr_l^{0.35} \left(\frac{\dot{q}p}{\rho_v h_{lv} g \mu_l \rho_l - \rho_v} \right)^{0.7}$ | Eq. (6) |
| Borishanskii-Mostinski | $\frac{\dot{q}^{0.3}}{\Delta T_s} = 0.1011 p_c^{0.69} (1.8 p_r^{0.17} + 4 p_r^{1.2} + 10 p_r^{10})$ | Eq. (7) |
| Shekriladze-Ratiani | $\frac{\dot{q}r_c}{k_l\Delta T_s} = 0.0122 \left(\frac{\dot{q}r_c^2 \rho_v h_{lv}}{\sigma k_l T_{sat}} \right)^{0.7} \left[\frac{\sqrt{p \rho_l (\rho_l / \rho_v - 1)} \sigma T_{sat} c_{p,l}}{\nu_l (\rho_v h_{lv})^2} \right]^{0.25}$ | Eq. (8) |
| Labuntsov | $\frac{\dot{q}^{1/3}}{\Delta T_s} = 0.075 \left[1 + 10 \left(\frac{\rho_v}{\rho_l - \rho_v} \right)^{2/3} \right] \left(\frac{k_l^2}{\nu_l \sigma T_{sat}} \right)^{1/3}$ | Eq. (9) |
| Gorenflo | $\frac{\dot{q}}{\Delta T_s} = 3580 \frac{W}{m^2 K} \left(\frac{\dot{q}}{20 \frac{kW}{m^2}} \right)^{0.95 - 0.3 p_r^{0.3}} \left(\frac{dp_s}{dT_s} \frac{1}{\sigma} \right)^{0.6} \left(0.7 p_r^{0.2} + 4 p_r + \frac{1.4 p_r}{1 - p_r} \right) \left(\frac{Ra}{0.4 \mu m} \right)^{2/15} \left(\frac{k_w \rho_w c_{p,w}}{1250 \frac{kJ^2}{m^4 K^2 s}} \right)^{0.25}$ | Eq. (10) |
| Stephan-Abdelsalam | $\frac{\dot{q}D_F}{k_l\Delta T_s} = 0.23 \left(\frac{\dot{q}D_F}{k_l T_{sat}} \right)^{0.674} \left(\frac{\rho_v}{\rho_l} \right)^{0.297} \left(\frac{h_{lv} D_F^2}{\alpha_l^2} \right)^{0.371} \left(\frac{\rho_l}{\rho_l - \rho_v} \right)^{1.73} \left(\frac{\alpha_l^2 \rho_l}{\sigma D_F} \right)^{0.35} \left(\frac{R_{p,DIN}}{1 \mu m} \right)^{0.133}$ | Eq. (11) |
| Cooper | $\frac{\dot{q}^{1/3}}{\Delta T_s} = 55 p_r^{0.12 - 0.2 \log R_{p,DIN}} (-\log p_r)^{-0.55} M^{-0.5}$ | Eq. (12) |
| Kutateladze | $\frac{\dot{q}L_c}{k_l\Delta T_s} = 3.37 \cdot 10^{-9} \left(\frac{c_{p,l}\Delta T_s}{h_{lv}} \right)^2 \left[\frac{(p/\rho_v)^2}{\sigma g / (\rho_l - \rho_g)} \right]$ | Eq. (13) |
| Leiner | $\frac{\dot{q}}{\Delta T_s} = 0.6161 p_c \left(\frac{\bar{R}}{MT_c} \right)^{1/2} \left[\frac{c_{p,l}(p_r = 0.1)M}{\bar{R}} \right]^{0.1512} \left[\frac{h_{lv}(p_r = 0.1)M}{\bar{R}T_c} \right]^{0.4894} 43000^{0.15 - 0.3 p_r^{0.3}} \left[1.2 p_r^{0.27} + \left(2.5 + \frac{1}{1 - p_r} \right) p_r \right] \left[\frac{\dot{q}}{p_c \left(\frac{\bar{R}T_c}{M} \right)^{1/2}} \right]^{0.9 - 0.3 p_r^{0.3}} \left[\frac{Ra}{\left(\frac{\bar{R}T_c}{N_a p_c} \right)^{1/3}} \right]^{0.133}$ | Eq. (14) |
| Pioro | $\frac{\dot{q}L_c}{k_l\Delta T_s} = C_{sf} \left[\frac{\dot{q}}{h_{lv} \rho_v^{1/2} [\sigma g (\rho_l - \rho_v)]^{1/4}} \right]^{2/3} Pr_l^m$ | Eq. (15) |

Both the Rohsenow and the Piro correlations require fitting constants based on the surface-fluid combination. Two strategies are followed for both correlations: first the correlation is assessed using parameters found in previous studies and secondly the parameters are fitted using the measurements of this study.

In the Rohsenow correlation, three parameters can be varied: C_{sf} , r and s . r and s are kept to their standard values of 0.33 and 1.7 respectively. For the heater configuration, a value of 0.0037 is used based on the measurements of Forrest et al. (2013) on an aluminium surface. A value of 0.0050 is used for the power module configuration, based on the work of Cao et al. (2019) for boiling on a copper surface. A least-squares fitting was used to determine the parameter based on the measurement performed on both configurations. Remarkably, the fitted parameter was equal for both configurations at 0.0051 after rounding to the fourth decimal.

Two parameters should be fitted for each surface-fluid combination in the Piro correlation: C_{sf}^* and m . No values for these parameters are available for FK-649. The values for another refrigerant, R-113, are used instead and are gathered from Piro et al. (2004b). For aluminium, values of 45620 and -2.35 are used for C_{sf}^* and m respectively, while for copper these parameters are equal to 168885 and -3.14 respectively. Using a least-squares fitting procedure, the following values were found for C_{sf}^* and m : 50111 and -2.29 for the aluminium boiling surface and 34405 and -2.13 for the copper boiling surface.

3.3. Performance parameters

The predictive performance of the correlations is determined by calculating the normalized mean absolute error (NMAE) in Eq. (16). This is the average value of the absolute deviation of the predicted value to the measured value, scaled to the measured value. The lower the NMAE, the closer the correlation matches the experiments. Another interesting parameter is the maximal normalized absolute error (NAE_{max}), which gives the maximal deviation of the correlation and is defined by Eq. (17).

$$NMAE = \frac{1}{N_m} \sum_{i=1}^{N_m} \frac{|\Delta T_{s,m,i} - \Delta T_{s,p,i}|}{\Delta T_{s,m,i}} \quad \text{Eq. (16)}$$

$$NAE_{max} = \max \left(\frac{|\Delta T_{s,m} - \Delta T_{s,p}|}{\Delta T_{s,m}} \right) \quad \text{Eq. (17)}$$

In these equations, N_m is the number of measurement points and the indices m and p indicate measured and predicted values respectively.

3.4. Results

A total of 91 measurements points is used in the assessment of the correlations. Fig. 1 shows the predicted surface superheat temperature as a function of the measured surface superheat temperature for the fifteen correlations. The corresponding NMAE for the different correlations is shown in Table 2.

Unsurprisingly, the fitted correlations (Rohsenow and Piro) perform best. Although Piro has two fitted parameters, it performs negligibly better than the Rohsenow correlation which only has one fitting parameter. The Rohsenow correlation also performs very well using parameters from literature for the same surface material and fluid combination. For the Piro correlation, parameters for another refrigerant were used, which results in highly diverging results. This indicates that the correlation cannot be used if no measurements for fitting or parameters for the required fluid-surface combination are available.

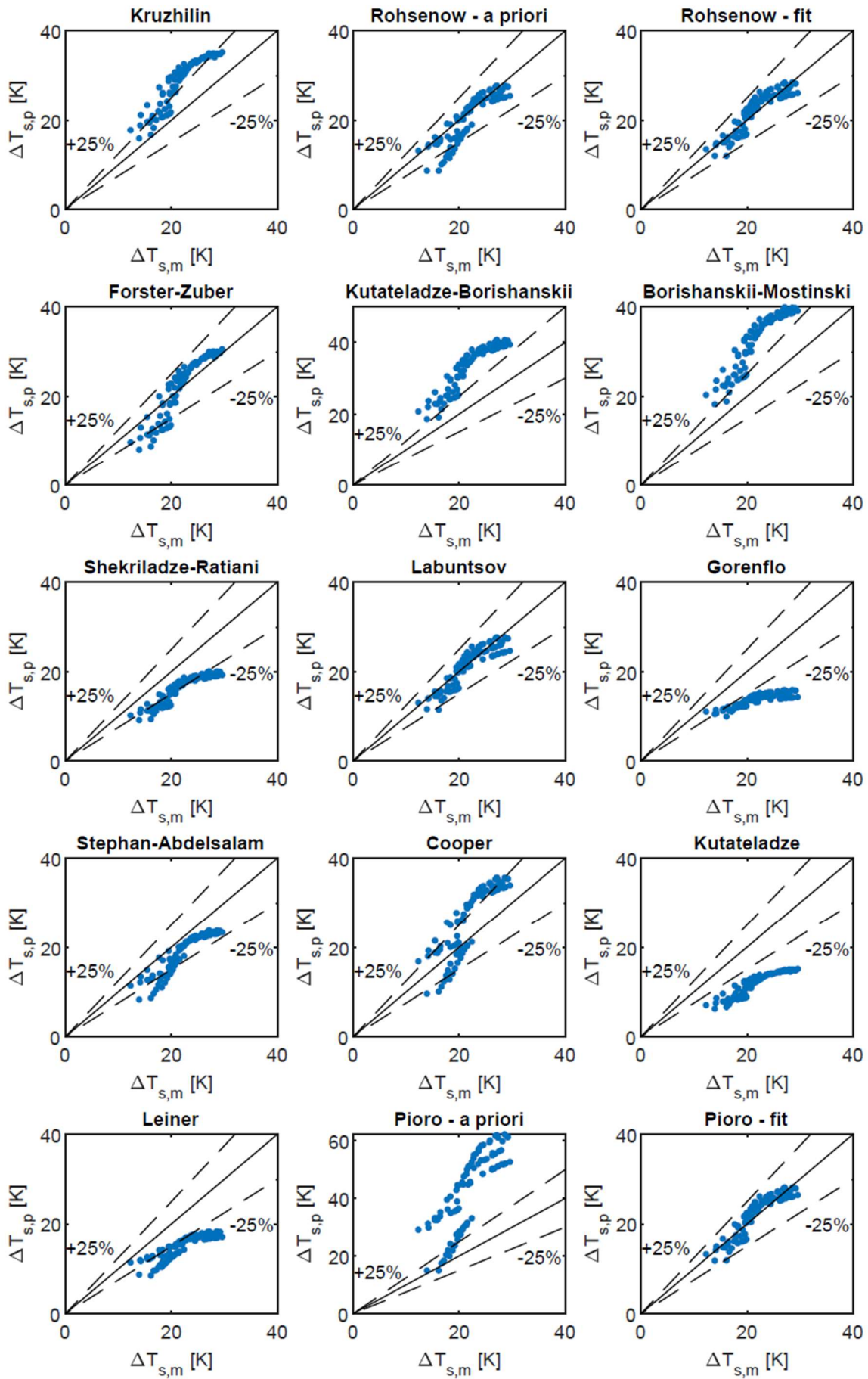


Figure 1: Predicted surface superheat temperature as a function of the measured surface superheat temperature for fifteen correlations.

Table 2. NMAE and NAE_{max} of the heat transfer correlations with regard to the experimental values

| Correlation | NMAE | NAE _{max} |
|--------------------------|-------|--------------------|
| Pioro - fit | 7.4% | 26.4% |
| Rohsenow - fit | 7.5% | 25.6% |
| Labuntsov | 7.5% | 29.1% |
| Rohsenow - a priori | 10.6% | 46.4% |
| Forster-Zuber | 13.7% | 45.9% |
| Stephan-Abdelsalam | 17.2% | 46.8% |
| Cooper | 25.2% | 44.6% |
| Shekriladze-Ratiani | 26.3% | 42.2% |
| Kruzhilin | 30.6% | 54.6% |
| Leiner | 31.7% | 47.4% |
| Gorenflo | 36.5% | 51.8% |
| Kutateladze | 45.6% | 59.2% |
| Borishanskii-Mostinski | 47.9% | 71.6% |
| Kutateladze-Borishanskii | 50.4% | 73.0% |
| Pioro - a priori | 94.8% | 142.5% |

Of the correlations without fitting constants, the Labuntsov correlation has the same NMAE as the fitted Rohsenow correlation, which is a very remarkable feat. It predicts all measurement points within 30%. For predicting the heat transfer rates of a fluid-surface combination which has not been tested, this correlation thus performs best. It should be noted that the Labuntsov correlation does not take into account the effect of the surface microgeometry, which is known to exist from multiple researches. Care should thus be taken to use the correlation for very smooth or rough surfaces, as this will hamper its predictive performance.

Next in line (after the Labuntsov and Rohsenow correlations) is the Forster-Zuber correlation. This result is quite unexpected, as this correlation is fitted to critical heat flux data and has a very diverging relation between heat flux and surface superheat temperature when compared to other correlations. The maximal deviation of all measurement points (45.9%) is however in line with most other correlations.

The Stephan-Abdelsalam, Cooper, Shekriladze-Ratiani, Kruzhilin, Leiner and Gorenflo correlations all have an NMAE ranging from 17% to 37% and a maximal deviation within 42% and 55%. These correlations are not quite able to properly predict the surface superheat temperatures measured in this study. The Kutateladze-Borishanskii, Borishanskii-Mostinski and Kutateladze correlations all have higher NMAE and maximal deviations. These correlations are not suitable to predict heat transfer rates for the conditions in this study.

4. CONCLUSIONS

Experimental measurements of nucleate pool boiling heat transfer of refrigerant FK-649 are compared to predictions by several correlations found in the scientific literature. The measurements were performed on two different boiling surfaces (aluminium and copper) with different roughness (0.9 μm and 0.2 μm) and both the heat flux and saturation temperature were varied, from 8 $\text{kW}\cdot\text{m}^{-2}$ to 146 $\text{kW}\cdot\text{m}^{-2}$ and from 36 °C to 46 °C respectively.

Out of the thirteen correlations selected, the Rohsenow correlation, which utilizes one fitting constant, and the Labuntsov correlation, which does not require any fitting constants, gave the best results in terms of predictive performance. Both correlations have a normalized mean absolute error of 7.5% when comparing the measurement data to the predictions, although the Labuntsov correlation had a slightly larger maximal deviation (29.1% compared to 25.6%). All other correlations had significantly higher normalized mean absolute errors and maximal deviations (ranging from 45.9% to 73.0%).

These results indicate that if there is no prior knowledge of the heat transfer rate for a specific surface-fluid combination, the Labuntsov correlation provides the best results. However, the Labuntsov correlation does not take into account the effect of boiling surface microgeometry, making it unsuitable for surfaces with very high or low surface roughness.

NOMENCLATURE

| | | | |
|--------------|--|--------------|---|
| C_{sf} | fitting parameter in Eq. (4) (-) | Pr_l | liquid Prandtl number (-) |
| C_{sf}^* | fitting parameter in Eq. (15) (-) | \dot{q} | heat flux ($W.m^{-2}$) |
| $C_{p,l}$ | liquid specific heat capacity ($J.kg^{-1}.K^{-1}$) | R_a | arithmetic mean surface roughness (m) |
| $C_{p,w}$ | wall specific heat capacity ($J.kg^{-1}.K^{-1}$) | $R_{p,DIN}$ | DIN 4762 surface roughness |
| D_F | Fritz bubble departure diameter (m) | r | fitting parameter in Eq. (4) (-) |
| g | gravitational acceleration ($m.s^{-2}$) | r_c | radius of the critical nucleus (m) |
| h_{lv} | latent heat of evaporation ($J.kg^{-1}$) | \bar{R} | universal gas constant ($8.31 J.mol^{-1}.K^{-1}$) |
| k_l | liquid thermal conductivity ($W.m^{-1}.K^{-1}$) | s | fitting parameter in Eq. (4) (-) |
| k_w | wall thermal conductivity ($W.m^{-1}.K^{-1}$) | T_c | critical temperature (K) |
| L_c | capillary length (m) | T_{sat} | saturation temperature (K) |
| M | molar mass ($kg.mol^{-1}$) | ΔT_s | surface superheat temperature (K) |
| m | fitting parameter in Eq. (15) (-) | α_l | liquid thermal diffusivity ($m^2.s^{-1}$) |
| NAE_{max} | max normalized absolute error (-) | β | static contact angle (rad) |
| $NMAE$ | normalized mean absolute error (-) | ν_l | kinematic viscosity ($m^2.s^{-1}$) |
| N_a | Avogadro constant ($6.022 \cdot 10^{23} mol^{-1}$) | μ_l | dynamic viscosity (Pa.s) |
| N_m | number of measurements (-) | ρ_l | liquid density ($kg.m^{-3}$) |
| p | pressure (Pa) | ρ_v | vapour density ($kg.m^{-3}$) |
| p_c | critical pressure (Pa) | ρ_w | wall density ($kg.m^{-3}$) |
| p_r | reduced pressure = p/p_c (-) | σ | surface tension ($N.m^{-3}$) |
| Δp_s | pressure difference related to ΔT_s (Pa) | | |

REFERENCES

- Bartle, R.S., Menon, K., Walsh, E., 2018. Pool boiling of resin-impregnated motor windings geometry. *Applied Thermal Engineering* 130, 854–864.
- Borishanskii, V.M., 1961. Accounting for the Effect of Pressure on Heat Transfer and Critical Heat Flux during Boiling Using the Theory of Thermodynamic Similarity. *Problems of Heat Transfer and Hydraulics in Two-Phase Media*, 18–36.
- Cao, Z., Wu, Z., Sundén, B., 2019. Heat transfer prediction and critical heat flux mechanism for pool boiling of NOVEC-649 on microporous copper surfaces. *International Journal of Heat and Mass Transfer* 141, 818–834.
- Cooper, M.G., 1984. Heat Flow Rates in Saturated Nucleate Pool Boiling-A Wide-Ranging Examination Using Reduced Properties. *Advances in Heat Transfer*, Elsevier, 157–239.
- Cui, J., Yan, S., Bi, S., Wu, J., 2018. Saturated Liquid Dynamic Viscosity and Surface Tension of trans-1-Chloro-3,3,3-trifluoropropene and Dodecafluoro-2-methylpentan-3-one. *J. Chem. Eng. Data* 63, 751–756.
- Forrest, E.C., Hu, L.-W., Buongiorno, J., McKrell, T.J., 2013. Pool Boiling Heat Transfer Performance of a Dielectric Fluid With Low Global Warming Potential. *Heat Transfer Engineering* 34, 1262–1277.
- Forster, H.K., Zuber, N., 1955. Dynamics of vapor bubbles and boiling heat transfer. *AIChE J.* 1, 531–535.
- Gorenflo, D., Kenning, D., 2010. *Pool Boiling*. VDI Heat Atlas, Springer Berlin Heidelberg, 757–792.
- Kruzhilin, G., 1947. Free-convection transfer of heat from a horizontal plate and boiling liquid. *Doklady AN SSSR (Reports of the USSR Academy of Sciences)* 58, 1657–1660.
- Kutateladze, S.S., 1990. *Natural Convection Boiling of Pure Saturated Fluids*. Heat Transfer and Hydrodynamic Resistance: Handbook, 197–200.

- Kutateladze, S.S., Borishanskii, V.M., 1958. Handbook on Heat Transfer.
- Labuntsov, D.A., 1972. Heat Transfer Problems with Nucleate Boiling of Liquids. *Teploenergetika* 19, 21–28.
- Leiner, W., 1994. Heat transfer by nucleate pool boiling—general correlation based on thermodynamic similarity. *International Journal of Heat and Mass Transfer* 37, 763–769.
- Lemmon, E., Bell, I.H., Huber, M., McLinden, M., 2018. NIST Standard Reference Database 23: Reference Fluid Thermodynamic and Transport Properties-REFPROP, Version 10.0, National Institute of Standards and Technology. Standard Reference Data Program, Gaithersburg.
- McLinden, M.O., Perkins, R.A., Lemmon, E.W., Fortin, T.J., 2015. Thermodynamic Properties of 1, 1, 1, 2, 2, 4, 5, 5, 5-Nonafluoro-4-(trifluoromethyl)-3-pentanone: Vapor pressure, (p, ρ , T) Behavior, and Speed of Sound Measurements, and an Equation of State. *Journal of Chemical & Engineering Data* 60, 3646–3659.
- Mostinski, I.L., 1963. Calculation of heat transfer and critical heat flux in boiling liquids based on the law of corresponding state. *Teploenergetika*, 10, 66–71.
- Perkins, R.A., Huber, M.L., Assael, M.J., 2018. Measurement and Correlation of the Thermal Conductivity of 1,1,1,2,2,4,5,5,5-Nonafluoro-4-(trifluoromethyl)-3-pentanone. *J. Chem. Eng. Data* 63, 2783–2789.
- Pirola, I.L., Rohsenow, W., Doerffer, S.S., 2004a. Nucleate pool-boiling heat transfer. I: review of parametric effects of boiling surface. *International Journal of Heat and Mass Transfer* 47, 5033–5044.
- Pirola, I.L., Rohsenow, W., Doerffer, S.S., 2004b. Nucleate pool-boiling heat transfer. II: assessment of prediction methods. *International Journal of Heat and Mass Transfer* 47, 5045–5057.
- Rohsenow, W., 1952. A Method of Correlating Heat-Transfer Data for Surface Boiling Liquids. *Transactions of the ASME* 74, 969–976.
- Shekriladze, I.G., 1981. Developed boiling heat transfer. *International Journal of Heat and Mass Transfer* 24, 795–801.
- Shekriladze, I., Ratiani, G., 1966. On the basic regularities of developed nucleate boiling heat transfer. *Bull. Acad. Sci. Georg. SSR* 42, 145–150.
- Stephan, K., Abdelsalam, M., 1980. Heat-transfer correlations for natural convection boiling. *International Journal of Heat and Mass Transfer* 23, 73–87.
- T’Jollyn, I., Nonneman, J., De Paepe, M., 2019. Pool boiling heat transfer measurements on a horizontal plate with a low global warming potential refrigerant. *Proceedings of the 25th IIR International Congress of Refrigeration (International Institute of Refrigeration)*, 1558–1564.
- T’Jollyn, I., Nonneman, J., Beyne, W., De Paepe, M., 2022. Nucleate pool boiling heat transfer and critical heat flux of FK-649 on an inverter power module. *Heat Mass Transfer*.
- Wen, C., Meng, X., Huber, M.L., Wu, J., 2017. Measurement and Correlation of the Viscosity of 1,1,1,2,2,4,5,5,5-Nonafluoro-4-(trifluoromethyl)-3-pentanone. *J. Chem. Eng. Data* 62, 3603–3609.